

Nuclear Halo and Molecular States

N.A. Orr

*Laboratoire de Physique Corpusculaire,
IN2P3-CNRS, ISMRa et Université de Caen,
14050 Caen Cedex, France*

Abstract.

Significant advances have been made in recent years in the exploration of clustering in light nuclei. This progress has arisen not only from the investigation of new systems, but also through the development and application of novel probes. This paper will briefly review selected topics concerning halo and molecular states in light nuclei through examples provided by the neutron-rich Be isotopes.

INTRODUCTION

Clustering within nuclei is a widespread phenomenon which takes on many guises across the nuclear landscape. Until relatively recently cluster studies have been confined to on or near the line of beta stability where the rôle of α -clustering has long been established [1]. As clustering is expected to manifest itself most strongly near thresholds [2], exotic structures might be expected to form in very neutron (or proton) rich systems. Over the last decade the exploration of clustering in nuclei far from stability has become technically feasible as demonstrated most clearly by the discovery and subsequent probing of the nuclear halo [3]. Whilst an excess of neutrons (or protons) may naively be expected to dilute any underlying α -cluster structures, theoretical [4,5] and experimental work [6,7] indicate that molecular type structures such as α -chains “bound” by valence neutrons may exist.

In the present paper a number of selected topics concerning the study of halo and molecular states in light, neutron-rich nuclei will be reviewed. As they exhibit many of the facets of clustering and structural evolution far from stability the neutron-rich Be isotopes have been chosen as examples. In parallel, the techniques which have been developed to aid in probing the structure of such nuclei far from stability will also be discussed.

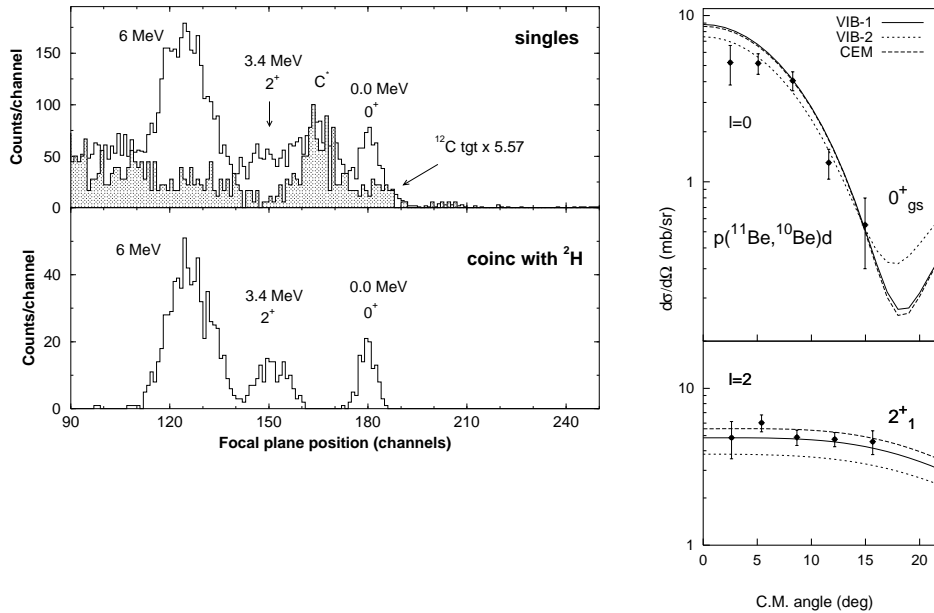


FIGURE 1. Left: Position spectra for ^{10}Be ions from the $p(^{11}\text{Be}, ^{10}\text{Be})d$ reaction on a $(\text{CH}_2)_n$ target. Right: Angular distributions for transfer to the ^{10}Be ground and 2^+ states. Comparison is made with various core coupling descriptions for ^{11}Be [10,11].

REACTION SPECTROSCOPY

Single-Nucleon Transfer Reactions

One of the issues of prime importance in the study of nuclei far from stability is the extraction of reliable spectroscopic information. For nuclei on or near stability light-ion (p , d , ...) induced single-nucleon transfer reactions have long been one of the tools of choice. The application of such reactions to nuclei far from stability presents a number of experimental challenges [8,9]. Most significantly, whilst the cross sections are moderately high ($\sim 1\text{-}10$ mb/sr) the short half-lives of the nuclei of interest dictate that beams of these nuclei be used in inverse kinematics reactions. The consequent constraints on the final excitation energy and angular resolution limit the target thickness to the order of 1 mg/cm 2 and beams of at least some 10^4 pps are required in order to obtain angular distributions in a reasonable measurement time.

A recent study [10,11] of the structure of the single-neutron halo nucleus ^{11}Be via the $p(^{11}\text{Be}, ^{10}\text{Be})d$ reaction at 35 MeV/nucleon provides a prototypical example of some of the features inherent in such reaction studies. Experimentally a magnetic spectrometer operated in a dispersion matched mode was employed to detect the heavy ejectile (^{10}Be). In order to remove the contamination arising from reactions on the C in the $(\text{CH}_2)_n$ target an array of large area silicon detectors was used to detect the coincident deuterons (figure 1). With a beam intensity of

$\sim 3 \times 10^4$ pps angular distributions of reasonable quality were acquired in some 72 hours of running (figure 1).

In addition to the experimental features illustrated by this experiment it should be stressed that the analysis is not model independent. For example, not only did the weakly bound nature of ^{11}Be and the d have to be taken into account but realistic wavefunctions had to be employed – here coupling to the strongly deformed ^{10}Be core needed to be properly accounted for. Indeed, the use of the standard separation energy approach to derive the radial form factors lead to an artificially high core excited state admixture. As detailed in refs [10,11], careful analysis indicates that the ground state of ^{11}Be is dominated (85%) by the admixture corresponding to the valence neutron occupying the $2s_{1/2}$ orbital together with a modest contribution (15%) from the core excited ($2^+ \otimes \nu 1d_{5/2}$) configuration.

Single-Nucleon Removal Reactions

Measurements of one-nucleon removal (or “knockout”) reactions on light targets have recently been proposed as a spectroscopic tool for high-energy radioactive beams [12,13]. This approach has arisen from the development of reaction calculations for halo nuclei in which the strong absorption limit [14] and core excited states are accounted for [13]. More specifically, the cross sections for the population of a given state of the core fragment (I_c^π) may be related to spectroscopic factors ($C^2S(I_c^\pi, nlj)$) using an extended version [13,15] of the spectator-core model [16] to calculate the cross section (σ_{sp}) for the removal of the nucleon (nlj).

$$\sigma(I_c^\pi) = \sum_{nlj} C^2S(I_c^\pi, nlj) \sigma_{sp}(nlj, S_n^{eff}) \quad (1)$$

The corresponding momentum distributions are derived within the same eikonal formalism [17] or in a simpler fashion using the opaque limit of the Serber model [18,19]. As noted above, the integrated cross sections for the population of the core excited states are directly related to the associated spectroscopic factors. In analogy with transfer reactions, the shape of the core fragment momentum distributions plays the rôle of the angular distributions in specifying the l of the removed nucleon. Experimentally the core fragment states are identified by the de-excitation γ -rays emitted in-flight, whilst a high acceptance magnetic spectrograph is used to determine the momenta.

One of the principal virtues offered by high energy nucleon removal is the applicability very far from stability where beam rates are low. This ability to function with intensities as low as 1pps is a consequence of the large cross sections (~ 10 - 100 mb), coupled with the high beam energies ($\gtrsim 40$ MeV/nucleon) which allow for the use of thick targets (~ 100 mg/cm²).

A particularly clear example¹ of the application of the technique may be found in the measurement of single-neutron removal from ^{12}Be [22], whereby the only

¹) Studies of other near dripline and halo nuclei may be found in ref's [12,20,21,23].

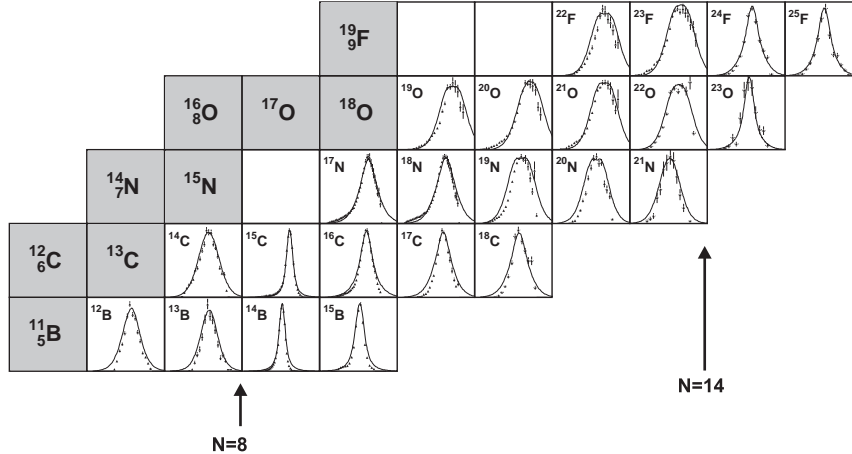


FIGURE 2. Core fragment longitudinal momentum distributions for one-neutron removal reactions on C. The solid lines correspond to Glauber model calculations [17].

bound core states are the ground ($J^\pi=1/2^+$) and 320 keV ($1/2^-$) levels in ^{11}Be . In simple terms, the population of the ^{11}Be ground state provides a measure of the $2\hbar\omega$ admixture present in ^{12}Be . The results of the experiment, which indicate only a $\sim 30\%$ admixture of the p^2 -configuration in ^{12}Be , provide direct confirmation [24,25] of the breakdown in the N=8 shell closure.

The potential power of the technique is further illustrated by a recent systematic investigation of a broad range of light, neutron-rich psd-shell nuclei [17]. The inclusive longitudinal momentum distributions which were obtained in a single rigidity setting are displayed in figure 2 whereby a number of features are immediately apparent. Most notably, the crossing of the N=8 shell and N=14 sub-shell closures are associated with a marked reduction in the widths of the core momentum distributions (viz, $^{14,15}\text{B}$, $^{15,16}\text{C}$, ^{23}O and $^{24,25}\text{F}$). The former effect arises from the large $\nu 2s_{1/2}$ admixtures expected in the ground states of the Z=4-6, N=9 isotones [23,26–28], which also persists for N=10, as suggested by recent studies of ^{14}Be [29,30] (see below). A narrowing of the momentum distributions may also be expected for N=15 and 16, as in a simple shell model picture the valence neutrons occupy the $\nu 2s_{1/2}$ orbital. Such results demonstrate that coupled with a high acceptance, broad range spectrograph, high energy single-nucleon removal reactions offer a powerful means to survey structural evolution over a wide range of isospin in a single experiment.

Finally, in the context of high energy reactions, it should also be noted, as described by Tostevin and Al-Khalili [15,31], that few-body Glauber model analyses of total reaction cross sections can also provide important constraints on the ground state wavefunctions of halo-like nuclei. As presented in the contribution to these proceedings by Suzuki, such analyses are now becoming more widespread in their application.

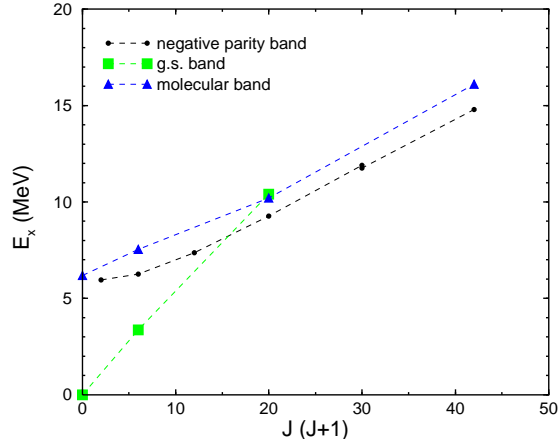


FIGURE 3. Spin-energy systematics for states observed in ^{10}Be (from [34]). The trajectories for the postulated positive and negative parity molecular bands are indicated.

NUCLEAR MOLECULAR CLUSTERS

As alluded to in the introduction, the α -particle plays an important rôle in the structure of light α -conjugate ($A=4n$) nuclei [1]. This is a direct consequence of the strongly bound character of the ^4He nucleus and the weakness of the α - α interaction, as evidenced by the unbound nature of ^8Be . The persistence of cluster structures for systems lying away from the line of beta-stability is well illustrated, as will be discussed here, by the beryllium isotopes, for which the α - α system may be regarded as the basis.

From a theoretical point of view, prescriptions such as the Molecular-Orbital Model (MO) [4] or the Two-Centre Shell Model (TCSM) [32], in which valence nucleons are added to the single-particle orbits arising from the two-centre potential, provide a successful means to describe the properties of these nuclei. Moreover these orbits may be viewed as the analogues of the σ and π -orbitals associated with the covalent binding of atomic molecules. The development of fully fledged Antisymmetrised Molecular Dynamics calculations (AMD) [5] is of particular interest as the N-nucleon system is modelled without any *a priori* imposition of an underlying cluster structure. Recent calculations, in particular, suggest the existence of two-centred structures in the Be, B and C isotopic chains with valence neutron density distributions exhibiting the features of molecular orbitals [5].

From an experimental perspective, von Oertzen [6] has compiled systematic evidence for the existence of dimers in $^9\text{--}^{11}\text{Be}$ and $^9\text{--}^{11}\text{B}$. In the case of ^9Be , for example, the presence of a valence neutron results in a bound (Borromean) system, the ground and excited states of which may be understood in terms of a three-body $\alpha:n:\alpha$ molecular structure. In particular, the rotational bands based on the ground and low-lying states exhibit large deformations consistent with the associated molecular configurations.

In the case of ^{10}Be , the experimental evidence for molecular configurations is

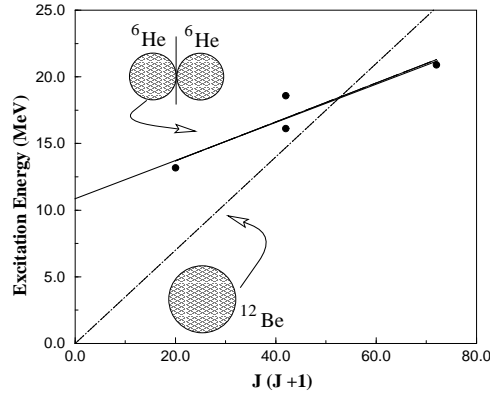


FIGURE 4. Spin-energy systematics for $^{12}\text{Be} \rightarrow ^6\text{He} + ^6\text{He}$ (from [7]).

rather less well documented. Beyond the established 0_2^+ , 2_2^+ and $1_1^- - 4_1^-$ states, the locations of the $J=5$ [6] and 6 members of the of the negative parity band, as well as the $J=4$ and 6 members of the positive parity band have been postulated following recent studies of the α - ^6He breakup of $^{10}\text{Be}^*$ [33,34]. As displayed in figure 3 [34], the spin-energy trajectories for the bands based on the 0_2^+ and 1_1^- states at ~ 6 MeV are consistent with large deformations as expected for molecular-like $\alpha:2n:\alpha$ structures. Moreover, the location of the bandheads just below the threshold for $\alpha + ^6\text{He}$ decay is in accordance with the considerations of Ikeda describing the formation of clusters [2]. Further support for the postulated molecular states may be found in the recent AMD calculations of Kanada-En'yo and collaborators [5], whereby well developed $\alpha:2n:\alpha$ configurations are predicted for the 0_2^+ and 1_1^- bands.

Given the existence of such molecular-type structures in ^{10}Be , the question naturally arises as to the existence of similar structures even further from stability. In this context the dripline nucleus ^{12}Be has been investigated. In a recent study² employing the inelastic excitation of an energetic (35 MeV/nucleon) secondary beam of ^{12}Be , evidence has been found in the breakup into $^6\text{He}+^6\text{He}$ of rotational states ($J=4, 6, 8$) in the excitation energy range 10-20 MeV [7]. As illustrated in figure 4, the inferred momenta of inertia ($\hbar^2/2\mathcal{I}=0.15\pm 0.04$ MeV) and bandhead energy (10.8 ± 1.8 MeV) of the observed states are consistent with the cluster decay of a molecular structure which may be associated with $\alpha:4n:\alpha$ configurations.

Further experimental support for the molecular nature of these states would be the observation of large spectroscopic factors for the associated clusters. The measurement of partial decay widths represents, however, formidable experimental challenges, though the presence of relatively few decay channels for the states in question may facilitate the measurements. Of additional interest is the search for in-band gamma transitions which should also furnish information on the degree of

²) The existence of such structures was hinted at in an earlier study by Korshennikov *et al.* [35].

clustering [36]. Such measurements may be possible in the near future through α -pickup reactions – such as $^{12}\text{C}(^{6,8}\text{He},^{10,12}\text{Be}^*)^8\text{Be}$ – carried out in conjunction with high efficiency charged particle and gamma arrays.

HALO STATES

Perhaps the most extreme form of clustering is that exhibited by halo nuclei, whereby one or more nucleons reside on average well beyond the core potential [3]. In the present discussion the two-neutron halo nucleus ^{14}Be will be used as an illustrative example. In particular, the spectroscopy of $^{13,14}\text{Be}$, continuum excitations of ^{14}Be and the spatial configuration of the halo neutrons will be addressed.

The tool chosen to investigate ^{14}Be in the work described here was a kinematically complete measurement of the fragments (^{12}Be and two neutrons) from the dissociation of a 35 MeV/nucleon beam of ^{14}Be on C and Pb targets. Such a measurement is now a relatively standard technique and allows the two-neutron removal cross sections, neutron angular distributions and invariant mass spectra to be extracted, and the neutron-neutron correlations to be explored.

The details of the experiment will not be repeated here as they have already been described in refs [29,37,38]. It should be stressed, however, that one of the principle problems confronting such measurements is the detection with the highest possible efficiency of two beam velocity neutrons at very forward angles with small relative momenta and minimal cross-talk. As described in refs [37,38], the use of a highly granular array arranged in a staggered configuration coupled with off-line cross-talk rejection algorithms (based on kinematic conditions) permit such measurements to be undertaken.

Structure and Continuum Excitations

The results obtained for the two-neutron removal cross sections, σ_{-2n} , the single-neutron angular distributions³, Γ_n , and the associated angle integrated cross sections, σ_n , are displayed in Table 1. The average neutron multiplicities ($\overline{m}_n = \sigma_n/\sigma_{-2n}$), which have also been deduced, are instructive in terms of the mechanisms leading to dissociation [39]. For a light target the reaction is expected to proceed via single-neutron removal (absorption or diffraction) followed by the in-flight decay of ^{13}Be . As approximately equal contributions are expected for absorption and diffraction [39] the average neutron multiplicity should be 1.5, in accordance with that measured. This scenario is also supported by the single-neutron angular distribution for the C target which is well reproduced assuming passage via a low-lying resonance in ^{13}Be [29,40]. In the case of a heavy target, nuclear and Coulomb dissociation occur. Given that Coulomb dissociation results

³) The angular distributions were well characterised by a Lorentzian lineshape.

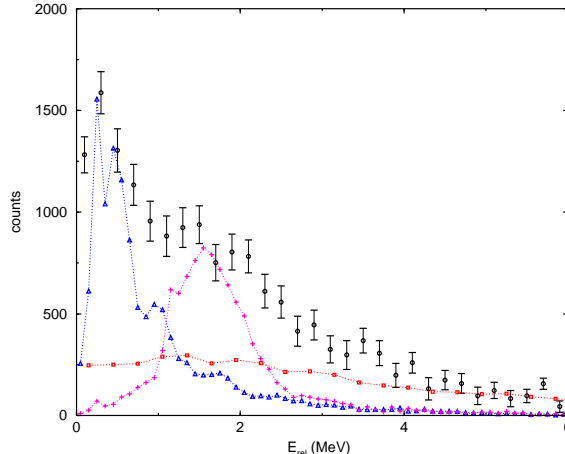


FIGURE 5. $^{12}\text{Be} + \text{neutron}$ relative energy spectrum from the dissociation of ^{14}Be on C at 35 MeV/nucleon [42]. The results of a simulation including states in ^{13}Be at 0.5 (triangles) and 2.0 MeV (crosses), with $\Gamma=0.5$ MeV are also displayed.

	σ_{-2n} [b]	σ_n [b]	\bar{m}_n	Γ_n [MeV/c]
C	0.46 ± 0.04	0.75 ± 0.10	1.6 ± 0.3	75 ± 3
Pb	2.3 ± 0.4	4.0 ± 0.3	1.7 ± 0.2	77 ± 4
Pb(EMD)	1.45 ± 0.40	2.7 ± 0.4	1.9 ± 0.6	87 ± 6

TABLE 1. Measured cross sections, average neutron multiplicities and neutron distribution momentum widths for the dissociation of ^{14}Be at 35 MeV/nucleon [29].

in a multiplicity of 2, the average multiplicity for dissociation on Pb should be between 1.5 and 2, as observed.

The possible existence of a low-lying state in ^{13}Be is of considerable importance in modelling the structure of ^{14}Be [41]; in particular in fixing the ^{12}Be -n interaction. Beyond the single-neutron angular distributions, the relative energy for $^{12}\text{Be} + n$ events may be reconstructed from the measured momenta. The preliminary results of such an analysis [42] are displayed in figure 5 together with the results of Monte Carlo simulations (see below) in which levels at 0.5 and 2.0 MeV above threshold are assumed with widths of $\Gamma=0.5$ MeV. The level at 2.0 MeV is that observed in multi-nucleon transfer reaction studies [43,44], whilst the former is consistent with a preliminary result reported by the MSU group [45]. Given, as discussed above, the appearance of ground states dominated by a valence $\nu 2s_{1/2}$ configuration for the neighbouring N=9 isotones ^{14}B and ^{15}C [17,21,23], together with the predicted continuation of such an inversion for ^{13}Be [26], it appears that the ground state is most probably $J^\pi=1/2^+$. Analysis of the $^{12}\text{Be} - n$ angular correlations should shed further light on this conjecture.

The enhanced cross section for dissociation on the Pb target (Table 1) is indicative of a large EMD contribution. Assuming that the nuclear-Coulomb interference is small, the C target data may be scaled to estimate the nuclear contribution to

breakup on Pb [29]. Given a root-mean-square radius of 3.2 fm for ^{14}Be [30], $\sigma_{-2n}^{nucl}(\text{Pb}) = 0.85 \pm 0.07$ b and, consequently, $\sigma_{-2n}^{EMD}(\text{Pb}) = 1.45 \pm 0.40$ b.

The invariant mass spectra, reconstructed from the measured momenta of the beam and fragments (^{12}Be and two neutrons) from breakup, are displayed in figure 6a and b for the C and Pb targets. The EMD spectrum (figure 6c) has been deduced following subtraction of the estimated nuclear contribution to reactions on Pb and exhibits enhanced strength around 1.5 MeV decay energy (E_{decay}). Given the complex nature of the response function of the present setup, a detailed Monte Carlo simulation, including the influence of all nonactive materials, was developed based on the GEANT package [29]. The results shown in figure 6 were obtained following the descriptions for dissociation on C and Pb outlined above and after filtering through the simulation. In the case of the nuclear induced reactions only the lowest low-lying state in ^{13}Be ($E_0 = 0.5$ MeV, $\Gamma_0 = 0.5$ MeV) was assumed to be populated following the diffraction of one of the halo neutrons. The EMD was simulated under the assumption that the energy sharing between the ^{12}Be and the two neutrons was governed by 3-body phase space. As shown in figure 6c, the observed EMD decay energy spectrum could be reproduced assuming a Breit-Wigner lineshape with $E_0 = 1.8 \pm 0.1$ MeV and $\Gamma_0 = 0.8 \pm 0.4$ MeV. Furthermore, the corresponding simulations of the single-neutron angular distributions were in good agreement with those observed [29].

Thompson and Zhukov have examined ^{14}Be within the framework of a 3-body model in which the ^{12}Be core was treated as inert⁴ [41] and a number of trial wavefunctions developed. Based on the binding energy and matter radius of ^{14}Be , together with the known d-wave resonance at 2.0 MeV in ^{13}Be , two ^{14}Be wavefunctions were favoured (both of which required an s-wave state near threshold in ^{13}Be as suggested above): the so-called D4 wavefunction – 86% $\nu(2s_{1/2})^2$ and 10% $\nu(1d_{5/2})^2$; and C7 – 29% $\nu(2s_{1/2})^2$ and 67% $\nu(1d_{5/2})^2$. The EMD decay energy spectra calculated from the corresponding E1 strength functions [41] are compared in figure 6 with that of the empirical Breit-Wigner lineshape deduced from the measurements. The corresponding integrated two-neutron removal cross sections are 1.05 b (D4) and 0.395 b (C7) [41], compared to the measured value of 1.45 ± 0.40 b. Although the strength is predicted to be concentrated at a somewhat lower energy than that observed, a large $\nu(2s_{1/2})^2$ admixture to the valence neutrons wavefunction is favoured. This conclusion is also supported by the total reaction cross section measurement of Suzuki *et al.* [30] reported in these proceedings.

A microscopic cluster model has also been used to explore $^{13,14}\text{Be}$ [46]. In the case of ^{13}Be an s-wave state is predicted very close to threshold, whilst the energy of the d-wave resonance is well reproduced. Significantly, a strong E1 transition [$B(E1) \approx 1.2 \text{e}^2 \text{fm}^2$] centred at $E_{decay} = 1.5$ MeV is predicted in ^{14}Be , very close to the structure observed experimentally. Analysis of the corresponding energy surface suggests, however, that this transition is not associated with a true resonance [46]. Consequently, the enhanced strength observed near threshold in the EMD invariant

⁴) An inert core precludes, ab initio, the existence of any simple negative parity resonances.

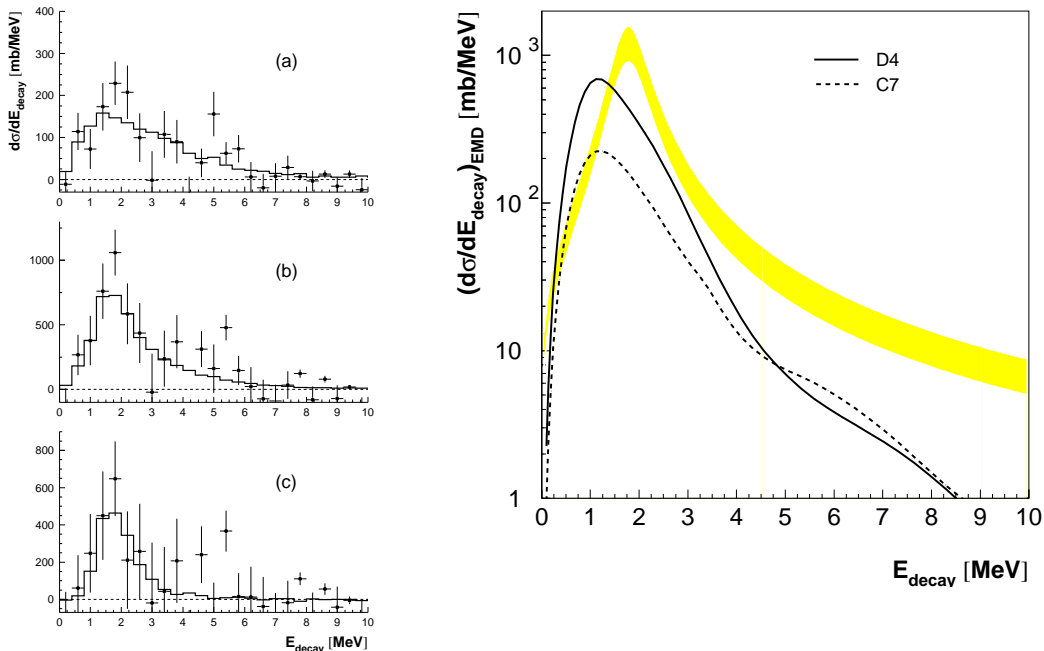


FIGURE 6. Left: Reconstructed decay energy spectra for the dissociation of ^{14}Be on (a) C, (b) Pb and (c) deduced for EMD on Pb. Right: Comparison of the EMD decay energy spectrum deduced from the measurement (shaded region) with 3-body calculations (see text).

mass spectrum may be qualified as a nonresonant “soft” dipole excitation.

In light of the breakdown in the neutron p-shell closure in ^{12}Be discussed previously, the importance of p-sd cross shell excitations in the ^{14}Be ground state should be explored. In a first instance, the search for core excited states ($^{12}\text{Be}^*$) in the dissociation of ^{14}Be may provide indications for the presence of such configurations, whilst theoretically the inclusion of a deformed core [25], in three-body calculations should be undertaken.

Neutron–Neutron Correlations

One of the most intriguing questions regarding the description of two-neutron halo systems is the degree of correlation between the neutrons. Considering only the intrinsic momentum distributions, a spatially compact dineutron will be characterised by $p_{\text{core}} = 2p_n$, whereas for a system with no correlations $p_{\text{core}} = \sqrt{2}p_n$. Unfortunately no unperturbed experimental measure of the momentum distributions is accessible.

Perhaps the method the most well adapted to probing spatial correlations is intensity interferometry [47]. In this approach the relative motion of the two outgoing neutrons is governed by the neutron–neutron final-state interaction and quantum statistics (Fermi-Dirac), both of which are related to the spatial characteristics of the source. Providing that any other effects on the neutron momenta may be ne-

glected or eliminated in the construction of the correlation function, interferometry provides a means to probe the spatial correlations of the halo neutrons [37].

Importantly, owing to the low momentum content of the halo neutrons, the standard approach to constructing correlation functions (applied, for example, in the measurement of Ieki *et al.* [48]) is no longer valid [38]. In particular, the narrow momentum distributions result in strong residual correlations and consequently a significant overestimate of the source size. As a result a new iterative technique has recently been developed and applied to the dissociation on a Pb target of beams of ${}^6\text{He}$, ${}^{11}\text{Li}$ and ${}^{14}\text{Be}$ [37]. Assuming that the timescale between the emission of the two neutrons was short ($\tau_{nn} \lesssim 100$ fm/c), as is most probably the case for EMD, neutron-neutron RMS separations of 5.9 ± 1.2 (${}^6\text{He}$), 6.6 ± 1.5 (${}^{11}\text{Li}$), and 5.4 ± 1.0 fm (${}^{14}\text{Be}$) have been deduced. These results appear to exclude the presence of any significant dineutron configurations. By way of comparison it is interesting to note that the RMS proton-neutron distance in the deuteron is some 3.8 fm. Future high statistics experiments employing a well modelled system such as ${}^6\text{He}$ should allow the emission timescale and source sizes to be extracted simultaneously from the longitudinal and transverse neutron-neutron relative momenta as well as coherent analyses of the neutron-neutron and core-neutron correlations.

CONCLUSIONS

In this paper some of the facets of nuclear halo and molecular states in light nuclei have been reviewed. In particular, various illustrative examples provided by the neutron-rich beryllium isotopes have been discussed. In addition, a number of related experimental probes have also been presented. Clearly no single technique can furnish a complete description of these nuclei and it will require the application of a broad range of theoretical and experimental tools to obtain a better understanding of the phenomena outlined here.

It is a pleasure to thank my colleagues in the Groupe Exotiques at LPC and in the DEMON, CHARISSA and E264/281/295 collaborations who have contributed to the work described here.

REFERENCES

1. M. Freer, A. Merchant, J. Phys. **G23** (1997) 261
2. K. Ikeda, Prog. Theor. Phys. (Japan) Supplement (1968) 464
3. P.G. Hansen, A. Jensen, B. Jonson, Ann. Rev. Nucl. Sci. **45** (1995) 591
4. M. Seya *et al.*, Prog. Theor. Phys. (Japan) **65** (1968) 205
5. Y. Kanada-En'yo *et al.*, Phys. Rev. **C60** (1999) 064304 and refs therein
6. W. von Oertzen, Z. Phys. **A354** (1996) 37; **A357** (1997) 355
7. M. Freer *et al.*, Phys. Rev. Lett. **82** (1999) 1383
8. J.S. Winfield, W.N. Catford, N.A. Orr, Nucl. Instr. Meth. **A396** (1997) 147
9. W.N. Catford, Proc. of RNBV, Nucl. Phys. A (in press)

10. S. Fortier *et al.*, Phys. Lett. **B461** (1999) 22
11. J.S. Winfield *et al.*, nucl-ex/0009015, Nucl. Phys. A (in press)
12. A. Navin *et al.*, Phys. Rev. Lett. **81** (1998) 5089
13. J.A. Tostevin, J. Phys. G: Nucl. Part. Phys. **25** (1999) 735
14. J. Hüfner, M.C. Nemes, Phys. Rev. **C23** (1981) 2538
15. J.A. Tostevin, Proc. of the 2nd Int. Conf. on Fission and Properties of Neutron-rich Nuclei (World Scientific, Singapore, 2000) p429
16. M.S. Hussein, K.W. McVoy, Nucl. Phys. **A445** (1985) 123
17. E. Sauvan *et al.*, nucl-ex/0007013, Phys. Lett. B (in press); E. Sauvan, Thèse, Université de Caen (2000), LPC Report LPCC T-00-01
18. P.G. Hansen, Phys. Rev. Lett. **77** (1996) 1016
19. H. Esbensen, Phys. Rev. **C53** (1996) 2007
20. T. Aumann *et al.*, Phys. Rev. Lett. **84** (2000) 35
21. V. Guimarães *et al.*, Phys. Rev. **C61** (2000) 064609
22. A. Navin *et al.*, Phys. Rev. Lett. **85** (2000) 266
23. V. Maddalena *et al.*, NSCL Report MSUCL-1171, August 2000
24. R. Sherr, H.T. Fortune, Phys. Rev. **C60** (1999) 064323 and refs therein
25. H. Iwasaki *et al.*, Phys. Lett. **B481** (2000) 7
26. Z. Ren *et al.*, Z. Phys. **A357** (1997) 137
27. D.E. Alburger, D.R. Goosman, Phys. Rev. **C10** (1974) 912
28. F. Ajzenberg-Selove, Nucl. Phys. **A449** (1986) 1
29. M. Labiche *et al.*, nucl-ex/0006003; M. Labiche, Thèse, Université de Caen (1999), LPC Report LPCC T-99-03
30. T. Suzuki *et al.*, Nucl. Phys. **A658** (1999) 313
31. J. Al-Khalili, J. Tostevin, Phys. Rev. Lett. **76** (1996) 3903
32. J.M. Eisenberg, W. Greiner, *Nuclear Theory* (North Holland, Amsterdam, 1975)
33. N. Soić *et al.*, Europhys. Lett. **34** (1996) 7
34. M. Freer *et al.*, submitted to Phys. Rev. C
35. A.A. Korsheninikov *et al.*, Phys. Lett. **B343** (1995) 53; RIKEN Report AF-NP-175
36. Y. Alhassid *et al.*, Phys. Rev. Lett. **49** (1982) 1482
37. F.M. Marqués *et al.*, Phys. Lett. **B476** (2000) 219
38. F.M. Marqués *et al.*, Nucl. Instrum. Meth. **A450** (2000) 109
39. F. Barranco *et al.*, Phys. Lett. **B319** (1993) 387
40. F. Barranco *et al.*, Z. Phys. **A356** (1996) 45
41. I.J. Thompson, M.V. Zhukov, Phys. Rev. **C53**, 708 (1996); *priv. comm*
42. K.L. Jones, Thesis, University of Surrey (2000)
43. A.N. Ostrowski *et al.*, Z. Phys. **A343** (1992) 489
44. M. Belozyorov *et al.*, Nucl. Phys. **A636** 419 (1998) 419
45. M. Thoennessen, Proc. Int. School of Heavy-Ion Physics, 4th Course: Exotic Nuclei, Ed. R.A. Broglia, P.G. Hansen (World Scientific, 1998) p269
46. P. Descouvemont, Phys. Rev. **C52**, 704 (1995); *priv. comm*
47. D.H. Boal *et al.*, Rev. Mod. Phys. **62** (1990) 553
48. K. Ieki *et al.*, Phys. Rev. Lett. **70** (1993) 730